



## Targeted combinational therapy inducing mitochondrial dysfunction†

Cite this: *Chem. Commun.*, 2017, 53, 1281

Received 10th November 2016,  
Accepted 22nd December 2016

DOI: 10.1039/c6cc08977a

www.rsc.org/chemcomm

Weon Sup Shin,<sup>‡a</sup> Soon Ki Park,<sup>‡b</sup> Peter Verwilst,<sup>‡a</sup> Seyoung Koo,<sup>a</sup> Joung Hae Lee,<sup>c</sup> Sung-Gil Chi<sup>\*b</sup> and Jong Seung Kim<sup>\*a</sup>

**We report on a mitochondria-specific combinational theranostic agent, 1. This system contains a chlorambucil prodrug and an aggregation induced emission dye. In addition, compound 1 bears both an intracellular thiol-triggered moiety and a mitochondria targeting unit (triphenylphosphonium). Glutathione (GSH) is the most abundant thiol and its concentrations are significantly higher in a great number of cancer cell lines, compared to normal cells. The GSH-induced prodrug 1 upon activation releases chlorambucil and exhibits mitochondria targeted aggregation induced emission (AIE) fluorescence, resulting in cell apoptosis via the caspase pathway due to mitochondrial dysfunction.**

Despite significant advances over the last few decades, cancer is still one of the leading causes of mortality worldwide and is projected to remain so over the next few decades, as the population in the developed world ages.<sup>1</sup> Cancer chemotherapy has become a method of choice in the treatment of cancers, especially in support of surgery. It has found application both as pre-surgical treatment to reduce the invasiveness of the procedure and as adjuvant treatment to reduce the risk of cancer recurrence post tumor resection.

Conventional anticancer drugs are commonly associated with a number of drawbacks, including lack of specificity, causing well known side effects due to significant toxicity in the skin, hair follicles, gastrointestinal lining cells, liver and kidneys. Furthermore, other limitations are the relatively low tumor accumulation and innate or induced drug resistance. Often, suboptimal doses of these potent drugs need to be administered to lower side effects to acceptable levels.

Chlorambucil is a nitrogen mustard drug, currently employed in clinical practice, particularly in the case of chronic lymphocytic

leukemia (CLL).<sup>2</sup> Chlorambucil confers its toxicity through the crosslinking of DNA, with a preferred reaction at the *N*-7 of guanidine moieties, causing inter- and intra-strand linking,<sup>3,4</sup> resulting in halted DNA replication and double strand breaks. However, the off-target delivery of this type of nitrogen mustard results in mutagenic effects in healthy cells,<sup>5</sup> greatly increasing the risk of secondary malignancies.<sup>6</sup>

Mitochondria, the primary source of energy in the form of ATP in healthy oxygenated cells, are currently under intense investigation as highly sensitive targets for anticancer drug design because these organelles are associated with an increased membrane potential in cancer cells. This altered membrane potential has been utilized to target drugs to these mitochondria as large lipophilic cations, such as the triphenylphosphonium moiety, accumulate in these subcellular organelles with concentration enhancements of several hundredfold reported for lipophilic cation appended molecules.<sup>7–11</sup> As the lower mitochondrial membrane potential of non-malignant cells results in a significantly lower uptake of these cations, as compared to malignant cells, covalently bonded drugs conjugated with lipophilic cations represent a convenient approach to enhance the tumor specific toxicity of these drugs.<sup>7–11</sup>

A key advantage of theranostic drug delivery systems is the possibility of visualizing the intracellular localization of drugs,<sup>12</sup> a key parameter in gaining a more thorough understanding of the mechanisms underlying the induction of toxicity. Rather than attaching a fluorophore with no auxiliary biological function, the combination of a drug and a fluorophore in a single molecule represents an unmistakable advantage in the atom-efficiency of theranostic molecular drug delivery systems.

Aggregation induced emission (AIE) fluorophores, a class of fluorescent molecules with intrinsic fluorescence only in a self-assembled state, unlike most fluorophores,<sup>13–15</sup> are a clear example of efficient multiple purpose molecular components, since the mitochondrial delivery of these dyes in the aggregated state has been demonstrated to result in severe mitochondrial dysfunction, loss of membrane integrity and, ultimately, cell death.<sup>16–18</sup>

<sup>a</sup> Department of Chemistry, Korea University, Seoul 02841, Korea.

E-mail: jongskim@korea.ac.kr

<sup>b</sup> Department of Life Sciences, Korea University, Seoul 02841, Korea.

E-mail: chi6302@korea.ac.kr

<sup>c</sup> Korea Research Institute of Standards and Science, Daejeon 305-600, Korea

† Electronic supplementary information (ESI) available: Experimental procedures, <sup>1</sup>H and <sup>13</sup>C NMR and ESI-MS data, and co-localisation data. See DOI: 10.1039/c6cc08977a

‡ These authors contributed equally to this work.

In the present work, we describe the development of a new combinational prodrug, **1**, which contains the DNA cross-linking agent chlorambucil and a mitochondria targeted aggregation induced emission fluorophore. The malignancy-dependent potency of the drug conjugate was further improved by including a glutathione (GSH)-cleavable linker, with demonstrated preferential drug activation in cancerous cells, exhibiting increased intracellular concentrations of GSH *versus* non-malignant cells.<sup>19–21</sup> As an anti-oxidant agent, GSH plays an important role under normal physiological conditions by scavenging the reactive oxygen species (ROS), which generates mitochondrial damage and cell death.<sup>22</sup> However, elevated GSH in cancer cells imparts growth advantages and chemotherapeutic resistances to the early and late stage of cancer.<sup>22</sup>

The synthesis of theranostic drug delivery system **1** is described in Scheme 1. The *o*-phenol-decorated tetraphenyl derivative **5** was synthesized by a McMurry coupling of the corresponding diarylketone, followed by a Suzuki reaction with 2-hydroxyphenylboronic acid, as described before.<sup>18</sup> The scaffold was subsequently decorated with a propargyl group following a Williamson ether synthesis with propargyl bromide, yielding intermediate **4**. A condensation reaction with 2,2-dithioethanol in the presence of phosgene was followed by an EDC (1-ethyl-3-(3-dimethylaminopropyl)carbodiimide hydrochloride) coupling with chlorambucil, resulting in intermediate **2**. Finally, the targeting group was added using a copper catalyzed “click” reaction with an

azide decorated triphenylphosphonium moiety (**7**) resulting in the final target compound (**1**).

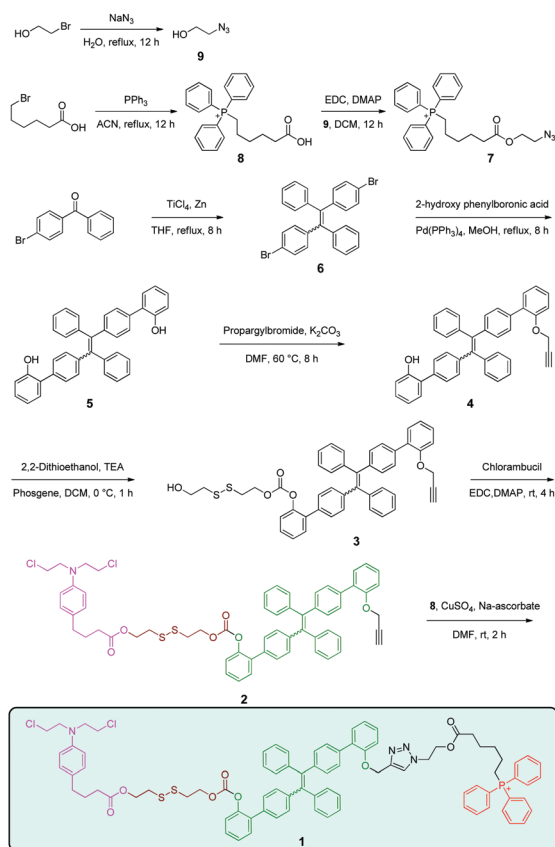
All new compounds (**1–4** and **7**) were characterized by <sup>1</sup>H and <sup>13</sup>C nuclear magnetic resonance (NMR) spectroscopy and electrospray ionization mass spectrometry (ESI-MS) and the results can be found in the ESI† (Fig. S1–S13).

The photophysical properties, stability of prodrug **1** as well as the reactivity in the presence of glutathione were investigated and the results are summarized in Fig. 1. The drug conjugate shows a maximum in absorbance around 320 nm in the UV/Vis spectrum in MeOH (Fig. 1a), whereas no fluorescence is detected under these conditions (Fig. 1b). With increasing amounts of water, the fluorescence is clearly increased, demonstrating a fluorescence spectrum centred around 490 nm. The increasing fluorescence in the case of increasing amounts of water clearly points to the aggregation induced emission effect as a mechanism to this observation, in accordance with previous results.<sup>18</sup>

Upon addition of an excess of glutathione, the HPLC chromatogram (Fig. 1c) clearly indicates the nearly complete activation of the drug after 60 minutes, with the disappearance of the peak with a retention time of 16 minutes. The addition of GSH results in the release of chlorambucil (retention time 14.7 minutes) as well as compound **10** (Fig. S14, ESI†), exhibiting a retention time of 18.5 minutes. The identity of the peaks was confirmed by ESI-MS (Fig. S14, ESI†).

Importantly, compound **1** did show a clear stability in the absence of added thiols, with no signs of decomposition of the probe in solution after 6 hours (Fig. 1d).

Probe **1** was added to two cell lines with different GSH levels; whereas normal NHDF cells exhibit a low intracellular GSH content, the cancerous PC3 cell line is characterized by a high



Scheme 1 Synthetic pathway towards **1**.

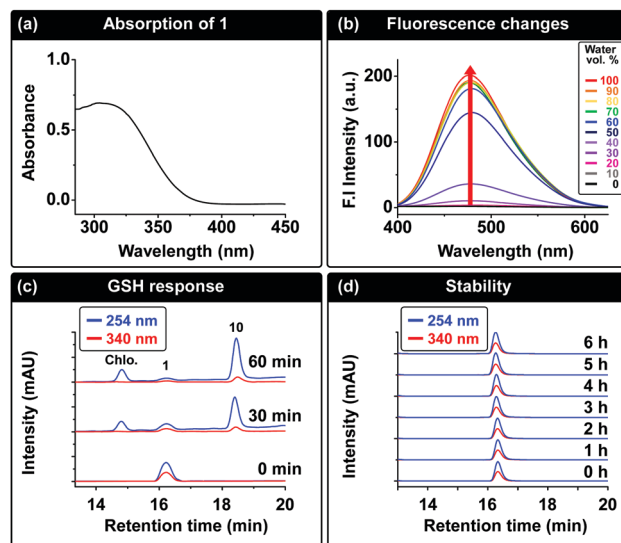


Fig. 1 Physicochemical properties of **1**. (a) Absorption of **1** (20  $\mu$ M) in pH 7.4 PBS solution at room temperature. (b) The dependence of water content (in methanol) on the AIE emission of **1** ( $\lambda_{\text{ex}}$  = 360 nm, slit = 3/3,  $T$  = 24  $^{\circ}$ C). (c) HPLC chromatograms in the presence of GSH and (d) in the absence of GSH at 37  $^{\circ}$ C for 6 h. Gradient: 70% B to 100% B for 17 min, then 100% B, 10 min; A: water, B: ACN.

intracellular concentration of this tripeptide.<sup>23</sup> The intracellular concentration of GSH is mirrored by the fluorescence observed for **1**-loaded cells, clearly demonstrating significantly enhanced fluorescence in the PC3 cells (Fig. S15, ESI<sup>†</sup>).

To assess the cytotoxic effect of compound **1**, two human cancer cell lines (HCT116; colon cancer, HeLa; cervical cancer) were treated with increasing doses of compound **1**, and the effects on cellular growth and viability were determined by cell counting and MTT assays. Compound **1** treatment led to a dose-associated reduction of cell numbers and showed a more drastic effect, compared to chlorambucil in all tested dose ranges (Fig. 2a and b). Consistently, MTT assays revealed that compound **1** causes a profound decrease in cell viability and evokes a much higher cytotoxic effect than chlorambucil (Fig. 2c and d). Intermediate **2**, not bearing the triphenylphosphonium targeting group, was used as a reference and showed only a slight reduction in viability in both cancer cells. Thus these results indicate that compound **1** has a more potent cytotoxic effect than chlorambucil and this effect depends on the mitochondria-targeting moiety.

The cytotoxicity of **1**, alongside several control compounds at a concentration of 20  $\mu\text{M}$ , was determined in NHDF (low GSH) and PC3 (high GSH) cells (Fig. S16, ESI<sup>†</sup>). Compound **1** is the only molecule that exhibits pathology associated differential toxicity. Precursor **2** and chlorambucil fail to exhibit any significant toxicity at this concentration, whereas compound **11** (ESI<sup>†</sup>), lacking the GSH trigger, proved to be universally toxic, in line with previous toxicity data on this molecule.<sup>18</sup>

Subsequently, the GSH-associated cytotoxicity of probe **1** was investigated. *N*-acetyl-*L*-cysteine (NAC) was used as a GSH inducer in HeLa cells. The cytotoxic effect of compound **1** was markedly increased by pre-incubation with NAC, while NAC

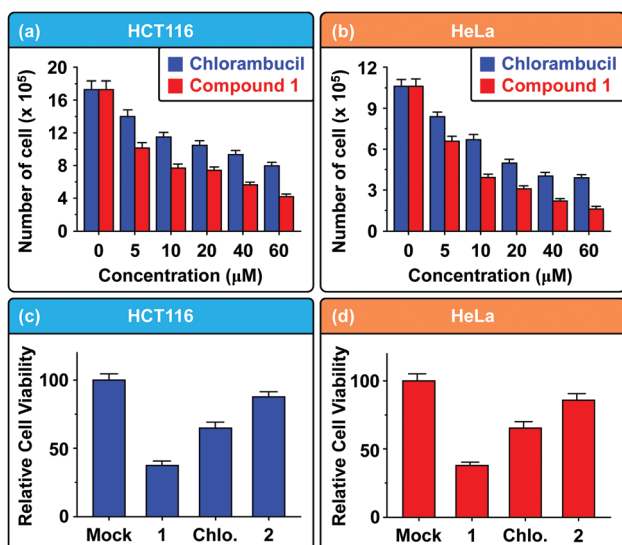


Fig. 2 Effect of compound **1** on the growth and viability of human cancer cells. (a and b) Comparison of the growth inhibition effect of compound **1** and chlorambucil in HCT116 (colon) and HeLa (cervix) cancer cells. Cells were counted after 24 h of treatment. (c and d) Comparison of compounds **1** and **2**, and chlorambucil on cell viability. MTT assays were performed after 24 h of treatment (20  $\mu\text{M}$ ).

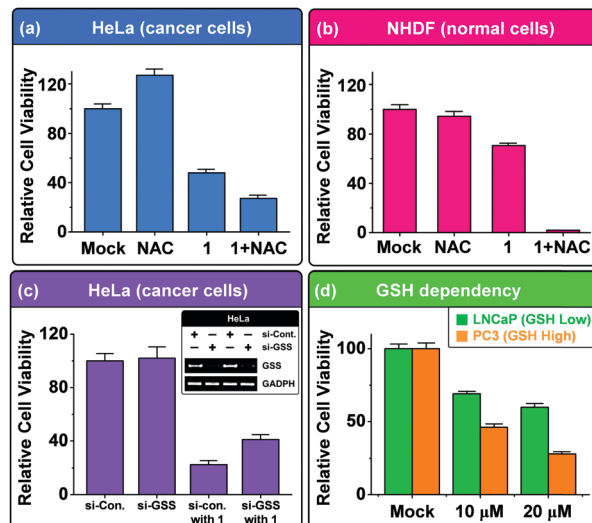


Fig. 3 The GSH-dependency of compound **1**'s effect on cell viability. (a and b) Enhancement of the cytotoxic effect of **1** in NAC-treated cells. NAC-untreated (Mock) or treated (1 mM) NHDF (normal) and HeLa (cancer) cells were incubated with compound **1** (20  $\mu\text{M}$ ) for 24 h. The cell viability was determined by an MTT assay. (c) The attenuation of compound **1**'s cytotoxic effect in GSS-depleted cancer cells. HeLa cells transfected with si-Control or si-GSS were incubated with compound **1** (20  $\mu\text{M}$ , 24 h). Inset: GSS content of siRNA treated cells. (d) Comparison of the cytotoxic effect of probe **1** in high and low GSH level cells. Two human prostate cancer cells expressing different levels of GSH (PC3, high GSH; LNCaP, low GSH) were treated with 10 or 20  $\mu\text{M}$  of compound **1** for 24 h.

itself (in the absence of probe **1**) rather enhances cell viability (Fig. 3a). Next, we compared its effect on the viability of normal cells (NHDFs; normal human dermal fibroblasts) in the absence and presence of NAC. As shown in Fig. 3b, compound **1** was significantly less potent in the normal cells, as compared to the cancerous HeLa cells; however, the addition of NAC resulted in a marked increase in toxicity. These results followed expectations as non-cancerous cells are known to exhibit far smaller intracellular GSH concentrations than many cancerous cells,<sup>19–21</sup> whereas the supplementation of NAC removed the differential GSH concentrations, thus significantly increasing the NHDF cell's sensitivity to drug conjugate **1**.

The GSH dependency on the toxicity was further studied using small interfering (si) RNA-mediated knockdown of glutathione synthetase (GSS), a key enzyme involved in GSH biosynthesis.<sup>19</sup> The knockdown of the GSS expression was verified by RT-PCR analysis of the GSS mRNA level (Fig. 3c inset). In accordance with the previous results, the cytotoxic effect of compound **1** was attenuated in HeLa cells by GSS depletion (Fig. 3c).

A final experiment to validate the proposed GSH-dependent cytotoxicity was performed using two human prostate cell lines (PC3 and LNCaP), exhibiting relatively high and low intracellular GSH levels, respectively.<sup>23</sup> As anticipated, a much stronger effect was observed in PC3 *versus* LNCaP cells (Fig. 3d). Together, these results clearly demonstrate that compound **1** exerts its cytotoxic effect in a GSH-dependent manner.

Mitochondrial dysfunction and DNA damage triggers apoptotic cell death to eliminate the abnormally damaged cells. Firstly, the

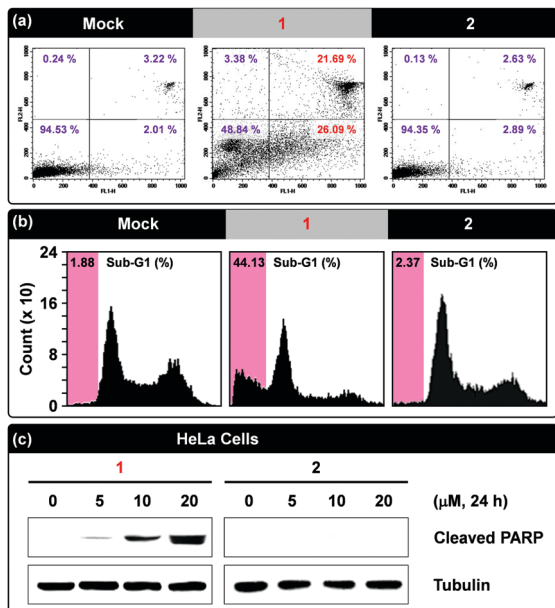


Fig. 4 Induction of tumour cell apoptosis by compound 1. (a) Annexin V assay showing the apoptosis-inducing effect of compound 1. HeLa cells were incubated with 20 μM of conjugate 1 for 24 h and Annexin V/PI double stained cells were analyzed by flow cytometry. (b) Flow cytometric analysis of the apoptotic sub-G1 fraction. HeLa cells were incubated with compound 1 or 2 (20 μM) for 24 h, and the percentage of the sub-G1 fraction was measured using flow cytometry. (c) Immunoblot assay of cleaved PARP. To confirm the apoptosis-inducing effect of 1, lysates of HeLa cells treated with 1 or 2 (20 μM, 24 h) were subjected to an immunoblot assay using a cleaved PARP-specific antibody.

mitochondrial localization of the AIE dyes was confirmed using confocal microscopy, demonstrating significant overlap with a MitoTracker dye (Fig. S17, ESI<sup>†</sup>). Secondly, to investigate whether compound 1 induces apoptosis, we performed flow cytometric analyses of annexin V expression and the apoptotic sub-G1 fraction. As shown in Fig. 4a and b, both annexin V-positive cell numbers and sub-G1 fractions were substantially increased by compound 1 treatment, while no detectable changes were observed in compound 2 treated cells. Consistently, an immunoblot assay showed that probe 1 treatment strongly induces PARP cleavage, a surrogate marker for apoptosis induction, while compound 2 shows no detectable effect (Fig. 4c). Therefore, these results support that the cytotoxic effect of compound 1 stems from its apoptosis-inducing activity.

As both mitochondrial alkylative DNA damage<sup>24</sup> and mitochondrial membrane disruption by AIE dyes<sup>16</sup> are known to result in increased ROS production, we hypothesize that the increased mitochondrial ROS production, in concert with the decreased GSH translocation into the mitochondrial matrix upon membrane damage,<sup>25</sup> results in the release of cytochrome c into the cytosol, initiating apoptosis *via* the intrinsic pathway.

In summary, we hereby report the new combinational therapeutic drug 1, which induces apoptotic cell death in a highly GSH-dependent manner. Considering the observed differential GSH

expression levels in cancerous cells, this effort to develop new drugs activated by intracellular GSH should give significant selectivity, with clear advantages for cancer chemotherapy. Our present study demonstrates that prodrug bearing theranostic 1 induces a cytotoxic effect selectively on naturally high GSH-expressing cancer cells by inducing mitochondrial dysfunction, DNA damage and subsequent apoptosis.

This work was supported by the Ministry of Science, ICT & Future Planning (MSIP) of the National Research Foundation of Korea (No. 2009-0081566 for JSK and NRF-20158A2A1A01005389 for SGC). This research was supported by the Korea Research Fellowship Program funded by the Ministry of Science, ICT and Future Planning through the National Research Foundation of Korea (2016H1D3A1938052 for PV).

## Notes and references

- 1 L. A. Torre, F. Bray, R. L. Siegel, J. Ferlay, J. Lortet-Tieulent and A. Jemal, *Ca-Cancer J. Clin.*, 2015, **65**, 87–108.
- 2 B. Eichhorst, M. Dreyling, T. Robak, E. Montserrat and M. Hallek, *Ann. Oncol.*, 2011, **22**(Suppl. 6), vi50–vi54.
- 3 W. B. Mattes, J. A. Hartley and K. W. Kohn, *Nucleic Acids Res.*, 1986, **14**, 2971–2987.
- 4 J. A. Hartley, J. P. Bingham and R. L. Souhami, *Nucleic Acids Res.*, 1992, **20**, 3175–3178.
- 5 B. J. Sanderson and A. J. Shield, *Mutat. Res.*, 1996, **355**, 41–57.
- 6 J. J. Castillo and M. A. Gertz, *Leuk. Lymphoma*, 2016, DOI: 10.1080/10428194.2016.1217527.
- 7 F. Wang, M. A. Ogasawara and P. Huang, *Mol. Aspects Med.*, 2010, **31**, 75–92.
- 8 S. Fulda, L. Galluzzi and G. Kroemer, *Nat. Rev. Drug Discovery*, 2010, **9**, 447–464.
- 9 R. A. Smith, R. C. Hartley and M. P. Murphy, *Antioxid. Redox Signaling*, 2011, **15**, 3021–3038.
- 10 S. R. Jean, D. V. Tulumello, S. P. Wisnovsky, E. K. Lei, M. P. Pereira and S. O. Kelley, *ACS Chem. Biol.*, 2014, **9**, 323–333.
- 11 Z.-P. Chen, M. Li, L.-J. Zhang, J.-Y. He, L. Wu, Y.-Y. Xiao, J.-A. Duan, T. Cai and W.-D. Li, *J. Drug Targeting*, 2016, **24**, 492–502.
- 12 R. Kumar, W. S. Shin, K. Sunwoo, W. Y. Kim, S. Koo, S. Bhuniya and J. S. Kim, *Chem. Soc. Rev.*, 2015, **44**, 6670–6683.
- 13 J. Mei, Y. Hong, J. W. Y. Lam, A. Qin, Y. Tang and B. Z. Tang, *Adv. Mater.*, 2014, **26**, 5429–5479.
- 14 R. T. Kwok, C. W. Leung, J. W. Lam and B. Z. Tang, *Chem. Soc. Rev.*, 2015, **44**, 4228–4238.
- 15 J. Mei, N. L. C. Leung, R. T. K. Kwok, J. W. Y. Lam and B. Z. Tang, *Chem. Rev.*, 2015, **115**, 11718–11940.
- 16 Q. Hu, M. Gao, G. Feng and B. Liu, *Angew. Chem., Int. Ed.*, 2014, **51**, 14225.
- 17 C.-J. Zhang, Q. Hu, G. Feng, R. Zhang, Y. Yuan, X. Lu and B. Liu, *Chem. Sci.*, 2015, **6**, 4580–4586.
- 18 W. S. Shin, M.-G. Lee, P. Verwilst, J. H. Lee, S.-G. Chi and J. S. Kim, *Chem. Sci.*, 2016, **7**, 6050–6059.
- 19 O. W. Griffith, *Free Radical Biol. Med.*, 1999, **27**, 922–935.
- 20 M. H. Lee, Z. Yang, C. W. Lim, Y. Lee, S. Dongbang, C. Kang and J. S. Kim, *Chem. Rev.*, 2013, **113**, 5071–5109.
- 21 M. H. Lee, J. L. Sessler and J. S. Kim, *Acc. Chem. Res.*, 2015, **48**, 2935–2946.
- 22 N. Traverso, R. Ricciarelli, M. Nitti, B. Marengo, A. L. Furfaro, M. A. Pronzato, U. M. Marinari and C. Domenicotti, *Oxid. Med. Cell. Longevity*, 2013, **2013**, 972913.
- 23 H.-W. Lim, S. Hong, W. Jin, S. Lim, S.-J. Kim, H.-J. Kang, E.-H. Park, K. Ahn and C.-J. Lim, *Exp. Mol. Med.*, 2005, **37**, 497–506.
- 24 M. Millard, J. D. Gallagher, B. Z. Olenyuk and N. Neamati, *J. Med. Chem.*, 2013, **56**, 9170–9179.
- 25 M. Mari, A. Morales, A. Colell, C. Garcia-Ruiz and J. C. Fernandez-Checa, *Antioxid. Redox Signaling*, 2009, **11**, 2685–2700.